Polymer 49 (2008) 5676–5682

Contents lists available at ScienceDirect

Polymer

journal homepage: www.elsevier.com/locate/polymer

Gelation behavior of polyacrylonitrile solution in relation to aging process and gel concentration

Lianjiang Tan [a], Ding Pan [a,*], Ning Pan [b]

[a] State Key Laboratory for Chemical Fibers Modification and Polymer Materials, Donghua University, Shanghai 201620, People's Republic of China
[b] Biological and Agricultural Engineering Department, University of California, CA 95616, USA

ARTICLE INFO

Article history:
Received 10 September 2008
Received in revised form 15 October 2008
Accepted 15 October 2008
Available online 22 October 2008

Keywords:
Polyacrylonitrile solution
Gelation
Rheological measurement

ABSTRACT

Polyacrylonitrile (PAN) was dissolved in dimethyl sulfoxide (DMSO) to prepare PAN solutions with various concentrations, and physical gel can form in PAN solution either after a long period of aging or at a low temperature, via physical cross-linking of PAN molecules. Through rheological measurements, we investigated the viscoelastic properties of the PAN solutions both at aging process and frequency scanning (given concentration and temperature). First based on the Winter and Chambon theory, we measured the critical gel time and the corresponding loss tangent tan δ for the PAN solutions during the aging processes. Then the critical gel concentration at different temperatures was examined by tracing the dynamic rheological parameters in frequency scanning tests. Difference was found to exist between the critical n values obtained in aging processes (0.74–0.76) and frequency scanning tests (0.64–0.65). Our results also showed that the power law relationships, i.e., $\eta_0 \propto \varepsilon^{-\gamma}$ and $G_e \propto \varepsilon^{z}$, are valid within experimental error for the PAN solutions before and beyond the gel point.

1. Introduction

Polymeric gel is a three-dimensional network, formed by flexible molecule chains either through chemical cross-linking or physical phase transformation [1]. During gelation, a polymer liquid (in many cases a polymer solution) gradually solidifies, and the liquid solution behaves more like an elastic solid beyond a critical point in terms of either aging time, polymer concentration, or temperature, etc. Dynamic rheology is a powerful tool to monitor gelation and microstructural changes in polymer materials [2], and the viscoelastic behavior of polymer gels near the sol–gel transition has been extensively studied [3–6]. The viscoelastic functions such as dynamic storage modulus G', loss modulus G'', loss tangent tan δ and complex viscosity η^* measured through dynamic shear tests are very sensitive to the structural changes during the formation of a polymer gel. It was reported that for many systems the crossover of G', and G'' is not a reliable criterion for determination of the gel point due to its high dependence on testing frequency, i.e., a crossover may occur at a fixed point by altering the testing frequency [7,8]. To bring the testing (angular) frequency ω into consideration, Winter et al. experimentally established a power law [9–11]

$$G'(\omega) \sim G''(\omega) \sim \omega^n \quad 0 < n < 1 \tag{1}$$

$$\tan\delta = G''(\omega)/G'(\omega) = \tan(n \cdot \pi/2) = \text{const} \tag{2}$$

for gelling systems, where the material constant n is the critical relaxation exponent *at the gel point*. The n value strongly depends on molecular and structural details of the system. It can be seen from Eq. (2) that when the gel point is such that $G' = G''$, there is $\tan\delta = 1$ and thus $n = 0.5$. However, the gel point of physical or chemical gels can also be achieved by altering the testing frequency so that $G' \neq G''$ and $\tan\delta \neq 1$, and consequently the n values were found to range over 0.5–0.75 [12,13] and even between 0.13 and 0.92 [14] at the gel point. Thus rather than using critical temperature as the only definition for the gel point, it is desirable and valid [2,15–17] that to define the gel point in terms of other variables involved as the critical gel concentration, time, frequency. A simple conversion between the time and frequency domains leads to a power law between the stress relaxation modulus and the time t *at the gel point* [18]:

$$G(t) \sim St^{-n} \quad (0 < n < 1) \tag{3}$$

where

$$G(t) = G'(t) + iG''(t), \quad t = \frac{2\pi}{\omega} \tag{4}$$

---

* Corresponding author. Tel.: +86 021 67792937.
E-mail addresses: dingpan@dhu.edu.cn, tanlianjiang@126.com (D. Pan).

0032-3861/$ – see front matter © 2008 Elsevier Ltd. All rights reserved.
doi:10.1016/j.polymer.2008.10.013

Here n is still the critical relaxation exponent and S is the gel strength which has an unusual dimension of Pa s^n. It turns out that Eq. (3) characterizes the gel point in such a way that it covers a large range over liquid and solid: stiffer gels at the critical point usually have a small n value ($0 \leftarrow n < 0.5$) and a larger strength factor S, while a larger n ($0.5 < n \rightarrow 1$) corresponds to a softer and more fragile gel with a smaller S [19]. Once above the gel point, stresses cannot relax completely and a finite value of the stress relaxation modulus, called the equilibrium modulus, exists:

$$G_e = \lim_{t\to\infty} G(t) \tag{5}$$

The main chemical characteristic of PAN is the presence of a permanent dipole in the monomer unit caused by the bulky CN group with strong polarity. This makes the gelation of PAN solutions possible if proper solvents are used (e.g. dimethyl formamide, dimethyl sulfoxide, etc.). Despite diverse gelation mechanisms, it is always possible to determine, atleast experimentally, the gel point and to assess the influences of all the related variables such as the polymer concentration, the aging temperature, and the addition of nonsolvent etc., since there are certain definitive relationships between the structure of gels, their rheological behaviors and these system parameters. In this article, we measured the rheological behaviors of PAN/DMSO solutions to investigate the viscoelastic properties of PAN gels during the aging process and the influence of the polymer concentration. The validity of the power law was also examined for gelation of the PAN/DMSO solution. Each rheological test was performed twice to reduce the experimental errors and ensure the reproducibility of the measurements.

2. Experimental section

2.1. Materials

PAN copolymers (acrylonitrile:itaconic acid = 98:2) were provided by Shanghai Institute of Synthetic Fiber with a viscosity-average molecular weight $\overline{M}_\eta = 7.8 \times 10^4$ g/mol^{-1}. DMSO (analytically pure) was purchased from Shanghai Wulian Chemical Industry Co. Ltd, and deionized water was used in the whole study.

2.2. Preparation of PAN solutions

Certain amounts of PAN copolymers were dispersed in a solvent (DMSO or the mixture of DMSO and water) in a three-neck bottle. The resulting slurry was left swollen at 50 °C for 2 h and at 60 °C for another 2 h, stirred by an electric paddle stirrer. Subsequently, it was stirred again at 70 °C for 6 more hours to produce a viscous PAN solution. Nine such PAN solutions with PAN concentrations from 15 wt% to 23 wt%, with an interval of 1 wt%, were prepared. Another two solutions containing 23 wt% PAN were also prepared, each with 2 wt% and 4 wt% water, respectively. The solutions were then deaerated for 3 h in a vacuum drying oven at 70 °C.

2.3. Rheological characterization

The dynamic rheological measurements were conducted using an advanced Solution and Melt Rotation Rheometer (ARES-RFS, TA, U.S.) equipped with two parallel plates. The temperature control was done with a thermostatic bath within ±0.1 °C of the preset

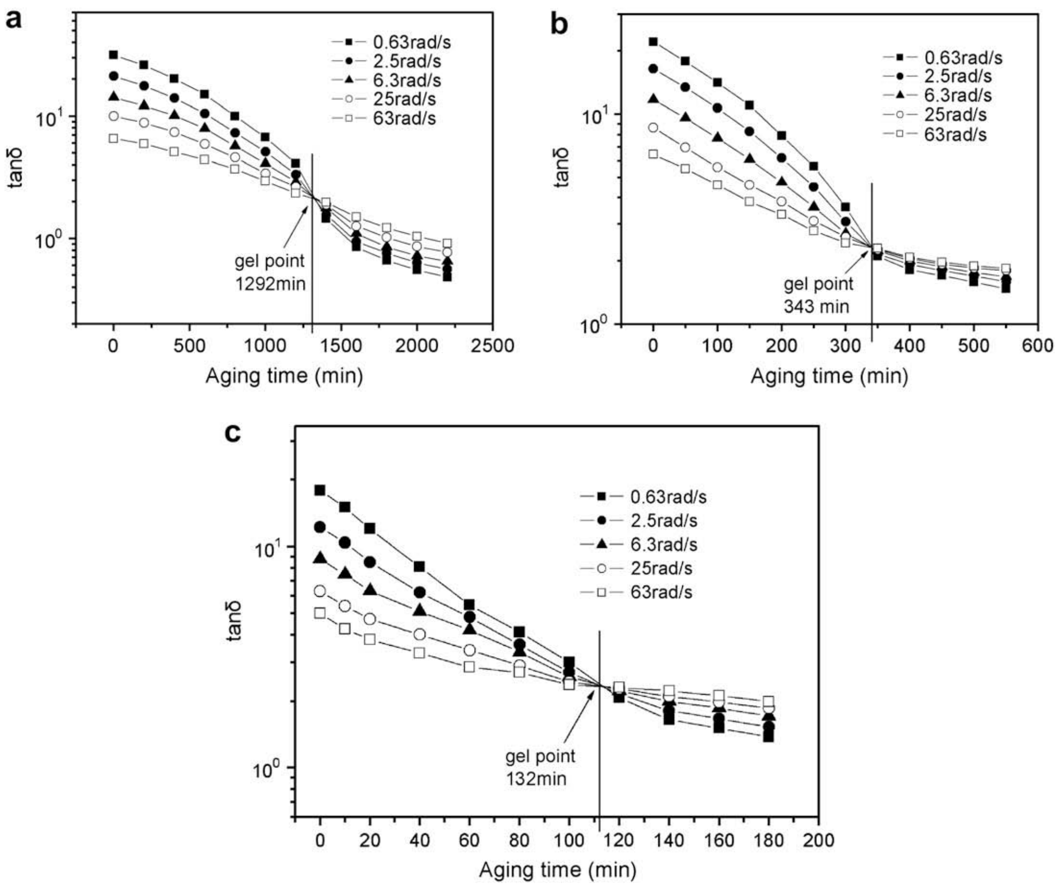

Fig. 1. The loss tangent tan δ versus aging time at various frequencies for 23 wt% PAN solutions (a) without water, (b) with 2 wt% water and (c) 4 wt% water. The aging temperature is 25 °C.

value. The parallel plate on which samples (the PAN solutions) were placed was 25 mm in diameter and the sample size was 2 mm. A thin layer of low-viscosity paraffin oil was applied to cover the samples, protecting them from dehydration or evaporation and thus minimizing the testing errors. 1% amplitude strain scanning at different temperatures in both sol and gel states of the samples were conducted to ensure the measurements done within a linear viscoelastic regime. For time scanning tests, five oscillation frequencies were first selected to trace the rheological parameters of the PAN solutions at a constant temperature of 25 °C. Then the same method was applied to the PAN solutions to obtain the loss tangent versus aging time relations at 10 °C, 0 °C, −10 °C and −20 °C, respectively. The frequency scanning tests were also conducted at frequency range from 100 rad/s to 0.1 rad/s. Each test was done after the PAN solution was conditioned at a desired temperature for 3 min so as to eliminate the influence of the thermal history. In all cases, fresh solutions were used immediately after deaeration in order to avoid gelation before the experiments.

3. Results and discussion

3.1. Gelation behavior of PAN solution during aging process

As largely as thermoreversible process, the gelation of PAN solution is very sensitive to temperature changes. Generally, the sol–gel transition of a PAN solution is ready to occur once the temperature decreases to a critical value T_g, and the reverse process (gel–sol transition or gel melting) happens when the temperature bounces back above T_g. Even the ambient temperature is sufficiently low, it will take a certain period of time, for the PAN solution to turn into a gel completely. This time is called the aging time t_a. Furthermore, the time point at which the gelation process starts is defined as critical gel time t_g. Both t_a and t_g have a close relationship with the degree of supercooling $\Delta T = T_g - T_a$, where T_a is the temperature after time t_a and termed the aging temperature. Obviously $\varDelta T$ reflects the temperature drop caused by the energy required for this sol–gel phase transition. On the other hand water as a nonsolvent for PAN can greatly promote the gelation of PAN solution, for it weakens the confinement of the solvent on the PAN molecular chains, by forming hydrogen bonds with the solvent molecules. Therefore, it is expected that increasing water content will shorten the aging time t_a and the critical gel time t_g. Based on our experience, the critical gelation temperature T_g of the 23 wt% PAN/DMSO solution without water was 53.3 °C in a temperature scanning test. So the temperatures chosen for the aging processes were much lower than 53.3 °C.

Winter et al. found that the relaxation exponent n is related to the fractal dimension of a polymer gel, which reflects the degree of compactness of the gel network [5,19,20]:

$$n = \frac{d_f}{d_f + 2} \tag{6}$$

where d_f is the fractal dimension of the polymer gel. Generally, a larger d_f value reflects a less compact and more irregular gel structure.

Table 1
Critical gel time t_g, loss tangent tan δ and critical relaxation exponent n for the three 23 wt% PAN solutions with different water contents (25 °C).

PAN solution	t_g (min)	tan δ	n	d_f
No water	1292	2.36	0.745	5.843
2 wt% water	343	2.42	0.751	6.032
4 wt% water	132	2.47	0.755	6.163

Table 2
Critical gel time t_g, loss tangent tan δ and critical relaxation exponent n for the 23 wt% PAN solution without water at different aging temperature.

T_a (°C)	$\varDelta T$ (°C)	t_g (min)	tan δ	n	d_f
25	28.3	1292	2.36	0.745	5.843
10	43.3	1073	2.46	0.754	6.130
0	53.3	908	2.44	0.752	6.065
−10	63.3	595	2.52	0.760	6.333
−20	73.3	358	2.41	0.750	6.000

We first examined the influence of water on the gelation by observing the changes of the dynamic parameters of PAN solutions caused by added water. In Fig. 1, the loss tangent tan δ was plotted against the aging time t_a for three 23 wt% PAN solutions with different water contents, and the tests were conducted at various oscillation frequencies ω. In general the plots show that, within each solution sample, the curves obtained under different oscillation frequencies converge at the same point of its corresponding t_g. Its critical relaxation exponent n as well as fractal dimension d_f can then be determined from the value of tan δ when $t = t_g$ and are listed in Table 1 together with the gel point t_g and tan δ.

As can be seen, it takes fairly long time ($\approx$21 h) for the solution to gel in the absence of water. Once water is added in, the gel time is significantly reduced to <6 h at 2 wt% water and <3 h at 4 wt% water, respectively. In other words, the more water added into the PAN solution, the quicker is the gel formation. The properties of the gels formed, as reflected from the critical relaxation exponent n and the fractal exponent, increase with the water content in the solution, albeit at much smaller rate than that of t_g. Furthermore, these properties still evolve with time beyond the gel point, at a smaller (than before) rate.

Next we investigated the influence of aging temperature on the gelation behavior of PAN solution for its obvious importance in practical applications. Besides at 25 °C, we measured the gel time t_g of the 23 wt% PAN solution without water at four additional aging temperatures T_a (10 °C, 0 °C, −10 °C, −20 °C), in the same way as above and shown in Table 2.

From Table 2 and the no-water result in Fig. 1(a), we find the critical gel time t_g increases with decreased aging temperature, i.e., it takes longer to gel at a higher temperature. The relationship between aging temperature and aging time is summarized in Fig. 2. When the temperature decreases below 0 °C, the gel time decreases more sharply, showing that the gelation process moves

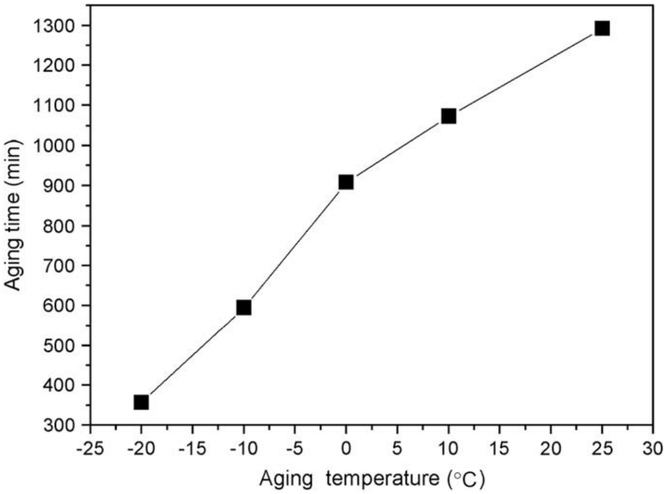

Fig. 2. The relationship between the aging time and aging temperature for the 23 wt% PAN solution without water.

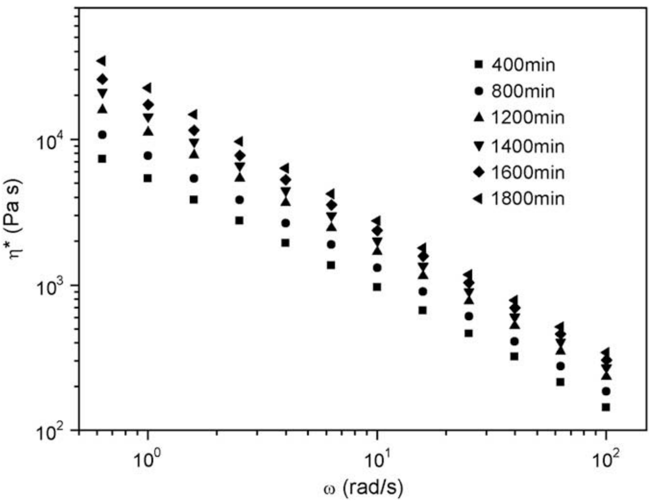

Fig. 3. The complex viscosity η^* versus frequency ω with aging time as the parameter for the 23 wt% PAN/DMSO solution without water (25 °C).

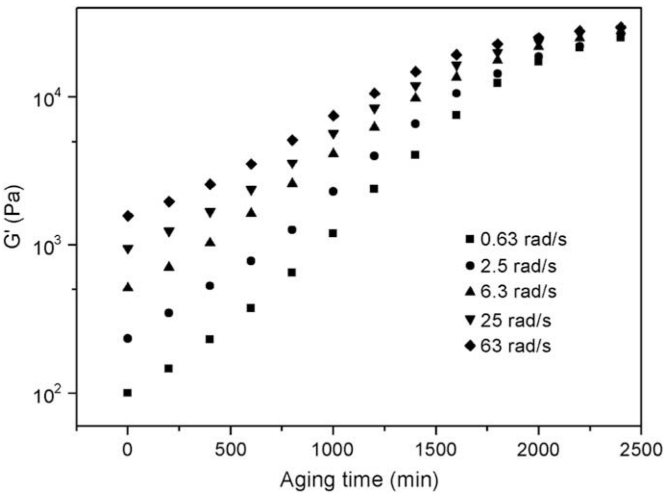

Fig. 5. The storage modulus G' versus aging time at various frequencies for the 23 wt% PAN/DMSO solution without water (25 °C).

much more rapidly below 0 °C. The n value and d_f value on the other hand change little and are very close to those obtained in Table 1, reflecting a similar gel structure irrespective of different PAN concentrations, water added and aging temperatures.

More quantitative description of the sol–gel transition is not easy due to the complexity of the phenomena. The introduction of power law at the gel point can greatly simplify this task [21]. The scaled dynamic properties such as zero-shear viscosity η_0 and equilibrium modulus G_e before and beyond the gel point respectively can be expressed as [19,22–25]:

$$\eta_0 \propto \varepsilon^{-\gamma}, \quad p < p_g \tag{7}$$

$$G_e \propto \varepsilon^{z}, \quad p > p_g \tag{8}$$

where $\varepsilon = |p_g - p|/p_g$ is the relative distance of a variable from the gel point p_g. γ is the power exponent determining the critical characteristics in the vicinity of sol–gel transition and governs the gelation rate. z is also a power exponent. γ and z can be calculated from the slopes of the G_e–ε plot and η_0–ε plot in log–log scale, respectively. p_g denotes the point where there is non-zero probability that a randomly chosen molecular chain exhibits infinite molecular weight [26]. For physical gels, p represents the extent of gelation and can be in terms of gel time, gelation concentration, gelation temperature, etc. While Eq. (8) serves well in the case of chemical gels, it should be used more carefully when physical gels are studied. G_e is in fact the quasi-equilibrium modulus, due to the extreme difficulty in obtaining the actual equilibrium modulus of physical gels [1]. The following relationship in this study is suggested:

$$\frac{p}{p_g} \approx \frac{t}{t_g} \tag{9}$$

and the expression of ε is thus:

$$\varepsilon = \left|t - t_g\right|/t_g \tag{10}$$

That is, when close to the gel point, the meaning of power law in terms of time should be the same as the percolation expressions (p and p_g) [21].

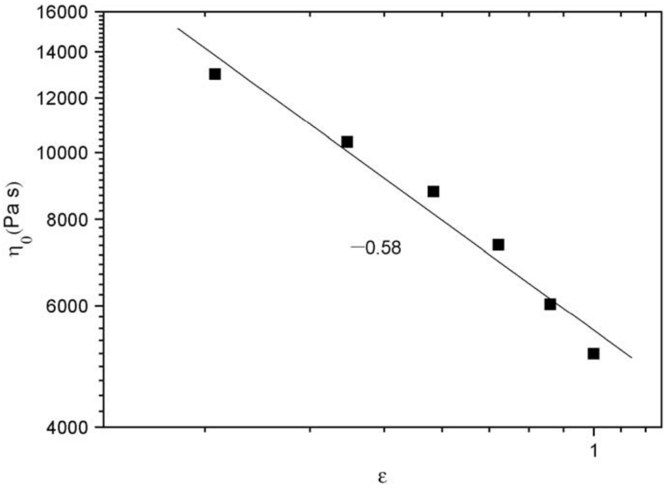

Fig. 4. The zero-shear viscosity η_0 versus the relative distance for the 23 wt% PAN/DMSO solution without water (25 °C).

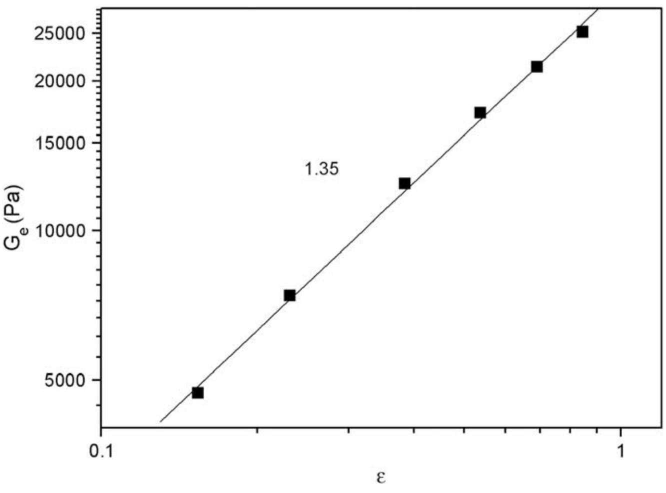

Fig. 6. The equilibrium modulus G_e versus the relative distance for the 23 wt% PAN/DMSO solution without water (25 °C).

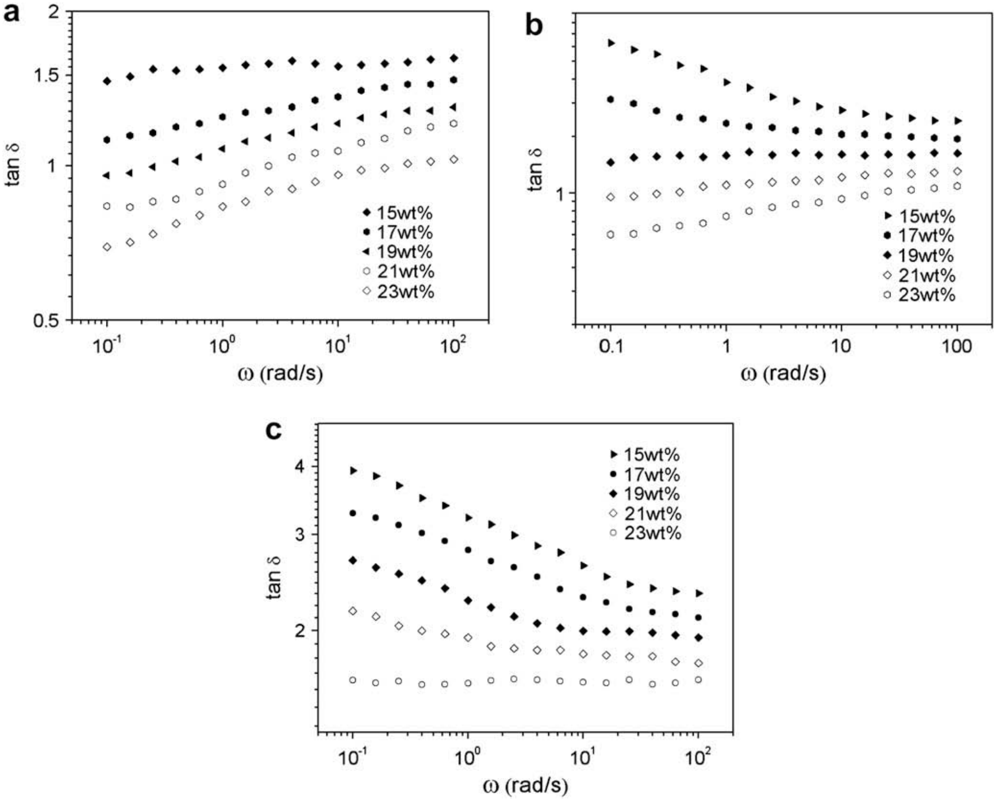

Fig. 7. The loss tangent tan δ as a function of frequency ω for the PAN solutions of various concentrations at (a) 38 °C (b) 45 °C (c) 53 °C.

Fig. 3 depicts the changes of the complex viscosity η^* with frequency at 25 °C for the 23 wt% PAN solution without water aged for different time. η^* is found to be the functions of both frequency and aging time. At a certain frequency, η^* increases with the aging time, indicating mutative viscoelastic properties of the solution. During the whole aging process, η^* decreases with increased frequency, typical of shear-thinning effect. The values of the zero-shear viscosity η_0 in Fig. 4 are the η^* values before the gel point at the frequency of 0.63 rad/s. This is valid as η^* becomes almost independent of the frequency when the frequency is below 1 rad/s. The linear fit of the η_0 values gives a slope of -0.58, i.e., $\gamma = 0.58$.

The evolution of the storage modulus G' during the aging process is shown in Fig. 5. The storage modulus started low and increases with the aging time, and its growing rate diminishes when approaching the gel point. G' still increases slightly beyond the gel point, as a consequence of cluster growth and gel formation, and shows only a little frequency dependence once elasticity dominates the system. Fig. 6 on the other hand shows the equilibrium modulus $G_e = \lim_{t\to\infty} G(t)$ as a function of ε beyond the gel point t_g. G' is in practice obtained from the end G' value at the frequency of 0.63 rad/s in Fig. 5, since a complete stress relaxation is more readily realized at a low frequency. The experimental data fall on a straight line with a slope of 1.35, that is, $z = 1.35$. A scaling relationship among the critical exponents has been suggested [6,18,27]:

$$n = z/(z+\gamma) \tag{11}$$

Based on the values of γ and z and Eq. (11), n turns out to be 0.7. Taking account of the experimental errors, this value agrees well with what determined from the tan δ versus aging time data.

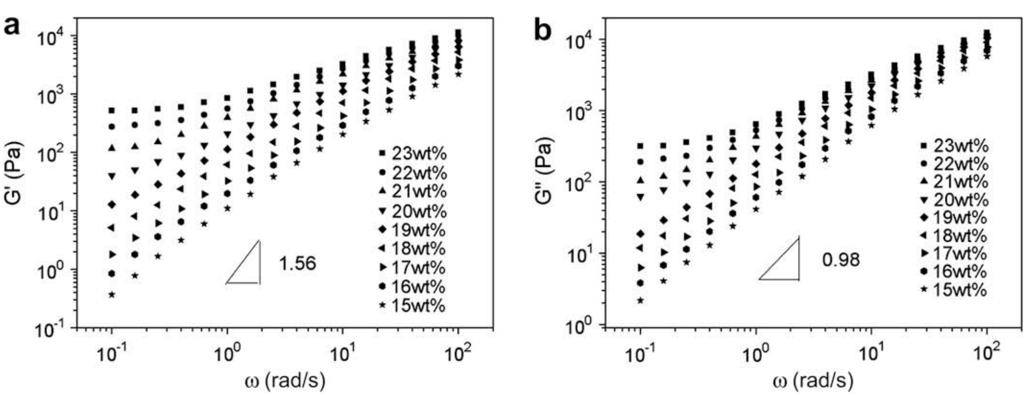

Fig. 8. Storage modulus G' (a) and loss modulus G'' (b) as functions of frequency ω for the PAN solutions of various concentrations at 45 °C.

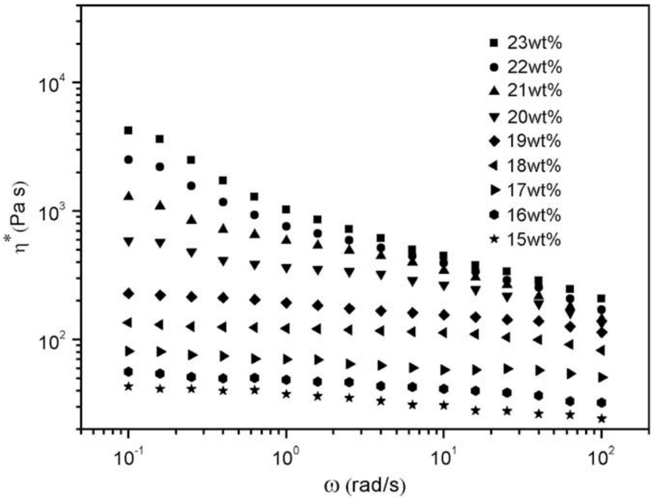

Fig. 9. The complex viscosity η^* as a function of frequency ω for the PAN solutions of various concentrations at 45 °C.

3.2. Gelation behavior of PAN/DMSO solution: critical gel concentration

tan δ as a function of ω for the PAN solutions of various concentrations and temperatures is shown in Fig. 7. tan δ value decreases with increase in concentration in all three cases, explained by a lower viscous/elastic ratio when the concentration is higher. At 45 °C, the tan δ curve of the solution with 19 wt% concentration exhibits certain frequency independence in the data range, indicating the occurrence of gelation at this concentration and temperature – it can thus be said that the critical gel concentration c_g at 45 °C is 19 wt% for the sample. The tan δ value of this curve is around 1.6, and the n value calculated accordingly is 0.644. The critical concentration values at two other temperature conditions 38 °C and 53 °C are $c_g = 15$ wt% and 23 wt%, respectively, i.e., c_g increasing with temperature. The n value however remains nearly constant (0.64–0.65) at different temperatures, irrespective of c_g. The fractal dimension d_f obtained from the n value based on Eq. (6) is therefore nearly unchanged, showing again the uniqueness of the PAN gel formed. The curves for the concentrations either higher or lower than the critical value c_g behave differently, since the solutions are either in gel or sol state.

As mentioned in last section, the n values of the gels formed during an aging process are around 0.75, larger than those just mentioned. This interesting finding shows that PAN gels formed in different conditions may have distinctive characteristics in structure. The focus here is the gel forming conditions. Aging at a temperature below the gelation temperature T_g tend to result in a PAN gel with lower strength (greater n value), while a PAN solution with the critical gel concentration c_g at a certain temperature undergoing frequency scanning gives a gel with a higher strength (smaller n value). Gelation of an aged solution needs a relatively long period of time, during which the fractal clusters gradually grow. The resultant gel structure thus tends to be more irregular and weaker, leading to larger n and d_f. Whereas gelation of a solution with critical concentration in frequency scanning process occurs within short time, giving rise to a more regular gel with higher strength. The phenomenon tells us that slow aging process may produce weaker gel, which should be avoided in fiber spinning and/or film casting.

G' and G″ versus frequencies at 45 °C are illustrated in Fig. 8. The selected concentrations range from 15 wt% to 23 wt%. Both G' and G'' exhibit a similar growing trend with either ω or concentration. At a given concentration, low frequencies correspond to smaller G' and G'', indicating polymer gels behave more like liquids. When the frequency increases, the gels become more like solids that G' and G'' keep growing and gradually become frequency insensitive. It is also noted that lower the concentration, more is the fluidic solution, the more frequency sensitive of the moduli. From the curves of the dynamic moduli for the solution of 15 wt% in Fig. 8, the slopes at very low frequency range were marked so there are:

$$G'(\omega) \sim \omega^{1.56} \quad G''(\omega) \sim \omega^{0.98} \quad (\omega \to 0) \tag{12}$$

The relationships $G'(\omega) \sim \omega^2$ and $G''(\omega) \sim \omega^1 (\omega \to 0)$ describes the liquid state of a viscoelastic sample [28]. The deviation from these relations reveals that the 15 wt% PAN solution has been in the process of gelation. It can also be observed that the slopes of the two curves G' and G'' take a similar value for the solution with 19 wt% concentration, showing 19 wt% is the critical gel concentration c_g at 45 °C, which is in agreement with Fig. 7.

The complex viscosity η^* is a variable useful in describing the viscoelastic properties of the gelation process. According to Muthukumar and Winter [29], the frequency dependence of the viscosity is shown to be:

$$\eta^*(\omega) \sim \omega^{-2/(d_f+2)}, \quad \omega > 0 \tag{13}$$

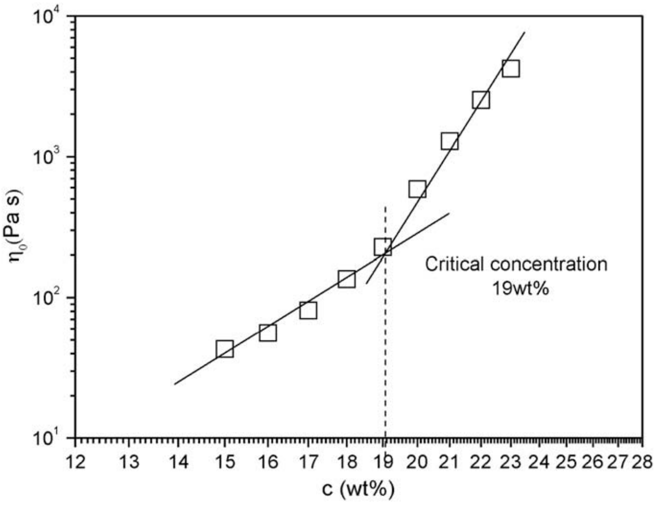

Fig. 10. η_0 obtained from Fig. 6 as a function of concentration at 45 °C.

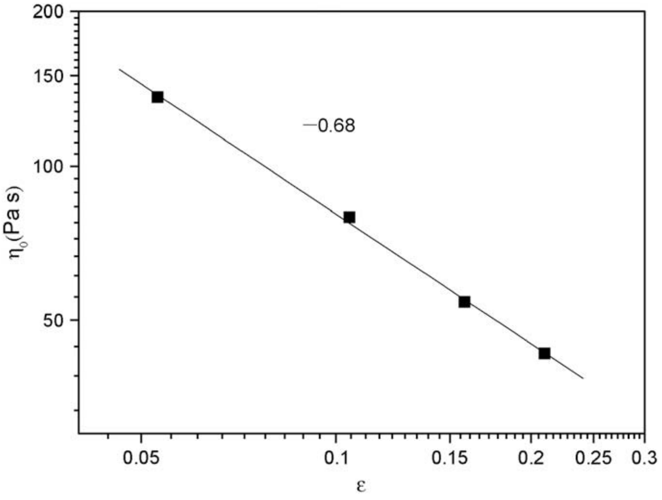

Fig. 11. η_0 as a function of the relative distance ε for the PAN solutions at 45 °C.

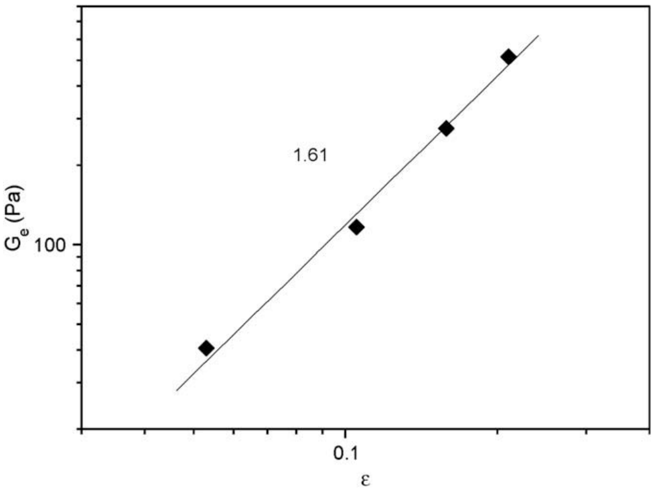

Fig. 12. G_e as a function of the relative distance ε for the PAN solutions at 45 °C.

where d_f is the fractal dimension as has been mentioned above. Since d_f is always positive, η^* is inversely proportional to ω. For many polymer solutions, the frequency dependence of η^* measured in oscillatory shear and that of apparent viscosity η_a in steady-state shear are observed to be closely related [30], when the numerical values of ω and $\cdot\gamma$ are comparable. The η^* versus ω data allow us to calculate the zero-shear viscosity. In Fig. 9, when ω is fixed, η^* increases as the concentration rises, mainly due to the aggregation of PAN molecules. On the other hand, at a given concentration level, η^* decreases with increased ω, suggesting the shear-thinning behavior of the PAN system in both sol and gel states. η^* is nearly frequency independent at extremely low frequencies, based on which the approximate value of zero-shear viscosity η_0 is determined.

The η_0 values versus concentration c at 45 °C are then plotted in Fig. 10. η_0 increases with concentration, again due to the enhancement of the aggregation of PAN in the solution. More importantly, the slope of this curve exhibits a break at the concentration of 19 wt%, the gel concentration c_g from both Figs. 7 and 8. This method can be employed to determine the critical gel concentration c_g by detecting the point where η_0 tends to diverge.

By now the critical gel concentration $c_g = 19$ wt% at 45 °C has been determined by both the G' and G'' versus ω curves, and the tan δ frequency-independence relation, and then further confirmed using the η_0–c curve. Using the known c_g value, we can once again calculate γ and z values. Here we use concentration c to replace the aging time t in Eq. (10) as:

$$\varepsilon = \left|c - c_g\right|/c_g \tag{14}$$

Fig. 11 shows η_0 as a function of the relative distance ε for the PAN solutions at 45 °C. The linear fitting of the data gives the slope value of −0.68, i.e., $\gamma = 0.68$. Fig. 12 gives G_e as a function of the relative distance ε for the PAN solutions at 45 °C. G_e has been obtained from the G' data at very low frequency (0.1 rad/s). The slope value of the linear fitting for this double logarithmic curve is $z = 1.61$. To validate the scaling relationship expressed by Eq. (11), the n value is calculated to be 0.703, and this result is comparable with that determined by the tan δ–ω relation, 0.644. Although discrepancy exists between the two values, we can still consider the power law to be feasible.

4. Conclusions

The gelation behavior of 23 wt% PAN/DMSO solutions during aging processes was first investigated. Adding water was found to accelerate the gelation of PAN solution, i.e., reducing the gel time t_g, and aging temperature will also significantly affect the gel time, which was especially apparent when the aging temperature fell below 0 °C. The value of the relaxation exponent n calculated using the power law relationship is in accordance with that obtained from the tan δ versus aging time data within experimental errors. The gelation behavior of PAN/DMSO solution as function of the PAN concentration has also been studied. The critical gel concentration varies at different temperatures. The power law also serves well for the solutions at 45 °C.

The critical exponent n value is different in the two experimental conditions: aging process and frequency scanning. In the aging process, the exponent n gave similar critical values (around 0.75) regardless of the water content and the aging temperature. Whereas in frequency scanning process, the n value obtained from the frequency-independent curve of the tan δ versus ω plot is in the range of 0.64–0.65, smaller than that obtained in the aging experiments. The disparity between the n values shows different critical structure and strength of the PAN gels formed in these two cases, which may be ascribed to the formation of a more irregular gel resulting from long-time structure evolution during the aging process.

Acknowledgements

This work was supported by grants from the National Basic Research Program (973 Program) (2006CB606505), the Shanghai Fundamental Theory Program (07DJ14002) and the Shanghai Leading Academic Discipline Project (B603).

References

[1] Lue Ang, Zhang Lina. J Phys Chem B 2008;112:4488.
[2] Madbouly SA, Otaigbe JU. Macromolecules 2005;38:10178–84.
[3] Muller R, Gerard E, Dugand P, Rempp P, Gnanou Y. Macromolecules 1991; 24:1321–6.
[4] Takahashi M, Yokoyama K, Masuda T, Takigawa T. J Chem Phys 1994;101:798–804.
[5] Muthukumar M. Macromolecules 1989;22:4656–8.
[6] Martin JE, Adolf D, Wilcoxon JP. Phys Rev A 1989;39:1325–32.
[7] Madbouly SA, Ougizawa T. J Macromol Sci Phys 2004;B43:471.
[8] Zhao Y, Cao Y, Yang Y, Wu C. Macromolecules 2003;36:855.
[9] Chambon F, Winter HH. J Rheol 1987;31(8):683–97.
[10] Chambon F, Winter HH. Polym Bull 1985;13:499–503.
[11] Te Nijenhuis K, Winter HH. Macromolecules 1989;22:411–4.
[12] Lairez D, Adam M, Emery JR, Durand D. Macromolecules 1992;25:286–9.
[13] Masataka S, Hirokazu H, Takashi T. Rheol Acta 2007;46:957–64.
[14] Scalan JC, Winter HH. Macromolecules 1991;24:47–54.
[15] Winter HH, Morganelli P, Chambon F. Macromolecules 1988;21:532.
[16] Kjoniksen A-L, Nystrom B. Macromolecules 1996;29:5252.
[17] Koike A, Nemoto N, Watanabe Y, Osaki K. Polym J 1996;28:942.
[18] Winter HH, Chambon F. J Rheol 1986;30:367.
[19] Winter HH, Mours M. Adv Polym Sci 1997;134:190.
[20] Hess W, Vilgis TA, Winter HH. Macromolecules 1988;21:2536.
[21] Cho Jaepyoung, Heuzey Marie-Claude. Colloid Polym Sci 2008;286:428.
[22] Stauffer D, Coniglio A, Adam A. Adv Polym Sci 1982;44:103–58.
[23] Zhang Y, Xu X, Xu J, Zhang L. Polymer 2007;48:6681–90.
[24] Wang Q, Li L. Carbohyd Polym 2005;62:232–8.
[25] Mours M, Winter HH. Macromolecules 1996;29:7221–9.
[26] Ross-Murphy SB. Polym Bull 2007;58:119.
[27] Winter HH. Prog Colloid Polym Sci 1987;75:104–7.
[28] Kobayashi K, Ching-I Huang, Lodge TP. Macromolecules 1999;32:7070–7.
[29] Muthukumar M, Winter HH. Macromolecules 1986;19:1284–5.
[30] Madbouly SA, Otaigbe JU, Nanda AK, Wicks DA. Polymer 2005;46:10897–907.